Published in
Journal of the Optical Society of America B 29, issue 10, 2944-2957, 2012
which should be used for any reference to this work

Cross-influence between the two servo loops of a fully stabilized Er:fiber optical frequency comb

Vladimir Dolgovskiy,* Nikola Bucalovic, Pierre Thomann, Christian Schori, Gianni Di Domenico, and Stéphane Schilt

Laboratoire Temps-Fréquence, Institut de Physique, Université de Neuchâtel, Avenue de Bellevaux 51, Neuchâtel 2000, Switzerland
**Corresponding author: vladimir.dolgovskiy@unine.ch*

We present a study of the impact of the cross-coupling between the two servo loops used to stabilize the repetition rate f_{rep} and the carrier-envelope offset (CEO) frequency f_{CEO} in a commercial Er:fiber frequency comb, based on the combination of experimental measurements and a model of the coupled loops. The developed theoretical model enables us to quantify the influence of the servo-loop coupling on an optical comb line, by simulating the hypothetic case where no coupling would be present. Numerical values for the model were obtained from an extensive characterization of the comb, in terms of frequency noise and dynamic response to a modulation applied to each actuator, for both f_{rep} and f_{CEO}. To validate the model, the frequency noise of an optical comb line at 1.56 μm was experimentally measured from the heterodyne beat between the comb and a cavity-stabilized ultranarrow-linewidth laser and showed good agreement with the calculated noise spectrum. The coupling between the two stabilization loops results in a more than 10-fold reduction of the comb mode frequency noise power spectral density in a wide Fourier frequency range.

1. INTRODUCTION

In the past decade, optical frequency combs have enabled impressive progress in numerous research areas, such as time and frequency metrology [1, 2] and broadband high-resolution spectroscopy [3–5], by providing a phase-coherent link between optical and microwave frequencies. The two parameters defining the frequency comb, i.e., the repetition rate f_{rep} and the carrier-envelope offset (CEO) frequency f_{CEO}, are both affected by a specific type of intra cavity perturbation, so that their noise is usually correlated [6,7]. Hence, for each intra cavity noise (such as environmental perturbations, pump-induced noise, or amplified spontaneous emission), there is one specific comb mode for which the resulting noise is minimized in the free-running comb. This has been previously described as a breathing motion of the comb around a so-called fixed point according to the elastic tape model introduced by Telle *et al.* [8]. In Telle *et al.*'s original model, as well as in subsequent experimental studies [9, 10], the fluctuations induced in f_{rep} and f_{CEO} by a given perturbation were implicitly assumed to be fully correlated (in phase) or anticorrelated (180° out-of-phase), so that the resulting noise cancels out at the fixed point. Here, we show from experimental data obtained in an Er:fiber comb that a different phase shift may occur between the response of f_{rep} and f_{CEO} to a given modulation. In that case, a true fixed point (at which the fluctuations induced by f_{rep} and f_{CEO} compensate exactly) does not exist and we introduce instead the concept of a quasi-fixed point at which the fluctuations induced in the optical comb line by f_{rep} are minimized by the fluctuations induced by f_{CEO}. We also show that this quasi-fixed point is not unique for a given source of perturbation but instead varies with the Fourier frequency of the perturbation, leading to a frequency-dependent quasi-fixed point.

Furthermore, the fixed point concept applies to a free-running comb only, and there has been little investigation of the impact of the correlation between f_{rep} and f_{CEO} in a fully stabilized comb so far. Full stabilization of a frequency comb is generally achieved using two phase-lock loops to coherently stabilize f_{rep} and f_{CEO} to a radio frequency (RF) reference [11]. Control of the laser cavity length using a piezoelectric transducer (PZT) is the traditional method of stabilizing the repetition rate, whereas the pump power is generally used to stabilize f_{CEO} [12,13]. However, these two actuators are not independent, and each of them has a simultaneous influence on the two comb parameters. Such behavior was predicted by the theory of Newbury and Washburn [14], but we report here precise experimental evidence of this effect. Similar transfer functions, including for femtosecond laser output power, have been reported for an Er:fiber frequency comb that makes use of an intracavity electro-optic modulator (EOM) for high-bandwidth stabilization of f_{rep} to an optical reference [15]. In that case, a strong focus was put on the comb dynamic response to the EOM modulation. Here, the target of our study is completely different, and our measured transfer functions for PZT and pump power modulation provide new insights into the noise of a free-running frequency comb. Furthermore, we demonstrate the first quantitative characterization of the impact of the coupling between the CEO and repetition rate servo loops in an Er:fiber comb stabilized to an RF reference. We observe an improvement of the frequency noise power spectral density (PSD) of an optical comb line by more than one order of magnitude over a wide

range of Fourier frequencies (100 Hz–10 kHz) resulting from this coupling. We introduce a theoretical model to describe the impact of the CEO servo loop on both the repetition rate and an optical comb mode. The good agreement observed between experimental results and calculated data validates our model.

The content of this paper is organized as follows. In Section 2, we briefly describe the frequency comb used in this study and the experimental methods applied to characterize its noise properties. In Section 3, we present the dynamic response of the comb measured for pump power and PZT modulation, and we introduce the concept of the frequency-dependent quasi-fixed point as an outcome of these measurements. Section 4 is devoted to the presentation of the model implemented to describe the coupled servo loops and its validation by experimental results showing the impact of the CEO servo loop on the noise of the repetition rate. In Section 5, this model is applied to quantify the impact of the servo-loop coupling on the frequency noise of a comb line. A conclusion is presented in Section 6. Finally, Appendix A contains a more exhaustive version of the model that takes into account the noise of the frequency references used in the stabilization loops.

2. EXPERIMENTAL METHOD

We used a commercial Er:fiber frequency comb (FC1500 from MenloSystems) in our experimental investigations. The comb is generated from a passively mode-locked fiber ring laser with a center wavelength of 1560 nm. The repetition rate is tuned to $f_{\mathrm{rep}} = 250$ MHz and is stabilized by feedback to a PZT that makes fine control of the laser cavity length. The error signal is generated by mixing down the fourth harmonic of f_{rep} (1 GHz) with a 980 MHz reference signal from a dielectric resonator oscillator (DRO) referenced to an H-maser. The resulting 20 MHz signal is compared to a stable reference signal from a direct digital synthesizer in a double-balanced mixer acting as an analog phase detector, whose output constitutes the error signal. This error signal is amplified in a proportional-integral-derivative (PID) controller (PIC210) and is fed back to a high-voltage amplifier with 23 dB gain that drives the PZT. Here we call u_{PZT} the input signal of the high-voltage amplifier.

The CEO beat is detected with a standard $f-2f$ interferometer [16] after spectral broadening of the laser output spectrum to one octave in a highly nonlinear fiber. Coarse tuning of the CEO frequency is performed by an intra cavity wedge, whereas fine tuning and stabilization are achieved by controlling the injection current of one of the pump diodes of the femtosecond laser. This is performed via a standard laser driver without any customization for fast pump power modulation as implemented in some cases [17]. The CEO beat frequency is phase-locked to a 20 MHz oscillator referenced to an H-maser. For this purpose, phase fluctuations between the CEO beat and the reference signal are detected in a digital phase detector (DXD200) with a large, linear detection range of $\pm 32 \cdot 2\pi$ phase difference. The resulting error signal is forwarded to a PID controller (PIC201) that drives the pump laser current source. We label u_{pump} the input signal that controls the pump laser driver.

In order to study the impact of the coupling between these two stabilization loops, we performed an extensive characterization of the comb in terms of frequency noise, dynamic response, and complete loop transfer functions, both for the repetition rate and the CEO beat. Furthermore, we also characterized the frequency noise and dynamic response of an optical comb line at 1.56 μm, by beating the comb with an ultranarrow-linewidth cavity-stabilized laser [18], to validate our model. Various frequency (phase) discriminators were used to demodulate the repetition rate, the CEO beat, and the heterodyne beat with the cavity-stabilized laser, in order to measure the frequency noise or the modulation response of these signals. A detailed description of these frequency discriminators has been previously reported together with their main characteristics [19]. In the present study, we mainly used a frequency discriminator based on a digital phase-lock loop (HF2PLL from Zurich Instrument) for the characterization of low-noise signals, e.g., for the repetition rate, and an RF discriminator with a broader frequency range (Miteq FMDM 21.4/2–4) for signals with a higher noise, such as the CEO beat or the comb–laser heterodyne beat. Frequency noise spectra were obtained by measuring the PSD of the discriminator output voltage using a fast Fourier transform (FFT) spectrum analyzer. The dynamic response of the comb to the modulation of the cavity length or of the pump power was obtained by synchronously detecting the output signal of the discriminator using a lock-in amplifier referenced to the modulation frequency.

3. FREQUENCY COMB DYNAMIC RESPONSE

In this section, we discuss the dynamic response of the comb, i.e., the response of f_{CEO} and f_{rep} experimentally measured for a modulation of the cavity length or pump power (Subsection 3.A). From these results, we extract new insights about the comb fixed point concept in Subsection 3.B.

A. Repetition Rate and CEO Dynamic Control

The two actuators used to control the CEO and the repetition rate in a frequency comb are not fully independent. A voltage applied to the PZT controlling the repetition rate also induces a shift of the CEO frequency, whereas the pump current influences both the CEO and the repetition rate frequencies. In order to quantify these coupled contributions, we measured four transfer function matrix elements determining the response of the comb to the various actuators as

$$\begin{pmatrix} \tilde{f}_{\mathrm{CEO}}(\omega) \\ \tilde{f}_{\mathrm{rep}}(\omega) \end{pmatrix} = \begin{pmatrix} C_{f_{\mathrm{CEO}} u_{\mathrm{pump}}}(\omega) & C_{f_{\mathrm{CEO}} u_{\mathrm{PZT}}}(\omega) \\ C_{f_{\mathrm{rep}} u_{\mathrm{pump}}}(\omega) & C_{f_{\mathrm{rep}} u_{\mathrm{PZT}}}(\omega) \end{pmatrix} \begin{pmatrix} \tilde{u}_{\mathrm{pump}}(\omega) \\ \tilde{u}_{\mathrm{PZT}}(\omega) \end{pmatrix}. \tag{1}$$

Here we define the Fourier transform of a function $u(t)$ by $\tilde{u}(\omega) = \lim_{T\to\infty} \int_{-T/2}^{+T/2} u(t) e^{i\omega t} \mathrm{d}t$. Throughout this paper, variables in the frequency (Fourier) domain are labeled with a tilde [e.g., $\tilde{u}(\omega)$], or by a capital letter [e.g., $C_{f_{\mathrm{CEO}} u_{\mathrm{pump}}}(\omega)$] in the case of transfer functions. The frequency dependence in the Fourier domain is denoted by the angular frequency ω to make the distinction from frequencies in the carrier domain that are labeled by f (e.g., f_{CEO} or f_{rep}).

First of all, the static tuning rates were determined by measuring the change in f_{rep} and f_{CEO} with respect to the DC voltage u_{pump} or u_{PZT} applied to the pump laser driver or to the PZT high voltage amplifier, respectively. The CEO and

repetition rate frequencies were measured with either an electrical spectrum analyzer or a frequency counter. The positive sign of the CEO beat frequency was unambiguously determined by observing the displacement of the beat frequency between one comb line and the 1.56 μm cavity-stabilized laser when f_{rep} and f_{CEO} were successively scanned. A linear regression of the frequency versus applied voltage was performed to extract the static tuning coefficients, which correspond to the local slope of the variation of f_{rep} (f_{CEO}) as a function of the control voltage u_{PZT} or u_{pump}. For a change of the cavity length, we obtained $\partial f_{CEO}/\partial u_{PZT} \approx -820$ kHz/V and $\partial f_{rep}/\partial u_{PZT} \approx 310$ Hz/V. For a change of the pump power, $\partial f_{CEO}/\partial u_{pump} \approx 110$ MHz/V and $\partial f_{rep}/\partial u_{pump} \approx -1.2$ kHz/V. The effect of a variation of the cavity length on the frequency of an optical comb line is strongly dominated by the contribution of the repetition rate, because of the large mode index ($N \approx 7.7 \cdot 10^5$ at $\lambda = 1.56$ μm) that multiplies the repetition rate. However, both the CEO and the repetition rate have a similar contribution to the tuning of a comb line with the pump laser power.

In addition to the static tuning rates, we also measured the dynamic response of f_{rep} and f_{CEO} to modulation of the pump power and of the cavity length. Such measurements show how the CEO and the repetition rate may be affected by external perturbations occurring at different frequencies, such as the noise on the pump laser current or mechanical noise induced by vibrations, air drafts, or temperature effects. The dynamic response (transfer function) of the repetition rate and CEO frequencies was measured by modulating the cavity length (via the PZT input voltage u_{PZT} with an amplitude of 100 mV rms) and the pump laser current (with a 10 mV rms amplitude applied to the current driver control voltage u_{pump}), respectively, with a sine waveform of varying frequency $\omega/2\pi$ (in the range from 0.1 Hz to 100 kHz) and by detecting the changes in f_{rep} and f_{CEO} occurring at the modulation frequency with a lock-in amplifier after demodulation. In order to observe the small frequency modulation (FM) induced on the RF carrier (f_{rep} or f_{CEO}), different frequency discriminators have been used to demodulate the frequency-modulated signals, as mentioned in Section 2. The discriminators operate around $f_{Discr} = 20$ MHz, but signals at a different frequency f_{signal} may be analyzed after frequency downconversion (by mixing with a reference signal at $f_{Discr} \pm f_{signal}$ and proper filtering). For example, due to the tiny variation of the repetition rate with the modulation signal (cavity length or pump current) compared to the corresponding effect on the CEO frequency, the detection has been performed at a high harmonic of the repetition rate in order to enlarge the frequency modulation depth to be detected by the frequency discriminator. For this purpose, the 12th harmonic of f_{rep} ($12 \times f_{rep} = 3$ GHz) has been detected using a fast photodiode (New-Focus 1434, 25 GHz bandwidth) and mixed with a reference signal at 2.98 GHz to produce the 20 MHz signal that was analyzed with either the Miteq or HF2PLL frequency discriminator. The analyzed signal thus contained 12 times the frequency modulation depth of f_{rep} and was later on scaled down by this factor in order to obtain the repetition rate transfer function. The output signal of the discriminator is proportional to the frequency modulation of the input signal and was subsequently analyzed with a lock-in amplifier to extract the component (in amplitude and phase) at the modulation frequency. Knowing the sensitivity of the frequency discriminator (in V/Hz) allowed us to convert the measured lock-in voltage into the frequency modulation. Our frequency discriminator has a sensitivity of 1.25 V/MHz for Miteq and is digitally adjustable for HF2PLL. A value in the range 10^{-3}–10^{-2} V/Hz was usually used with this discriminator. The bandwidth is about 2 MHz for Miteq and 50 kHz for HF2PLL [19].

The dynamic responses of f_{CEO} and f_{rep} to cavity length modulation are very different, as shown in Fig. 1(a). The PZT has many mechanical resonances that strongly affect the CEO response, especially above a few hundred hertz. We believe this effect to result from a tiny misalignment of the PZT from the optical axis, which induces changes in the polarization and amplitude of the pulses in the resonator via the complex laser dynamics. These resonances are only weakly visible on the repetition rate transfer function, which shows a cut-off frequency of a few kilohertz, whereas the CEO is affected by the PZT modulation up to a much higher frequency. The CEO and repetition rate tuning coefficients measured at low modulation frequency ($\omega/2\,\pi < 10$ Hz) are in relatively good agreement with the static values previously determined. Some difference is however observed, which can arise from the following two reasons: (i) between DC and 0.1 Hz, some slow physical phenomena (mainly of thermal origin) might occur and affect the dynamic response at very low frequency; (ii) the measurement of the static tuning coefficients might be affected by the drift of f_{CEO} and f_{rep} that arises in the free-running comb and which is difficult to distinguish from the deliberate frequency change induced by a change of the cavity length or pump current.

In a similar way, the CEO and repetition rate transfer functions were measured for pump power modulation. In addition to the analyzed change in the repetition rate frequency (FM signal), pump laser modulation also induces a modulation of the mode-locked laser optical power and thus an amplitude modulation (AM) of both the repetition rate and CEO beat signals. Due to the potential AM sensitivity of some frequency discriminators [19], great care was taken throughout the experiments to measure the true FM response of f_{CEO} and f_{rep} without being affected by residual AM effects. This was especially critical in the case of f_{rep}, as the FM depth is orders of magnitude smaller than for f_{CEO} and is thus more prone to AM-induced artifacts. For this reason, the dynamic response of f_{rep} has been measured by the digital phase-locked loop (PLL) discriminator HF2PLL, which proved to be affected only marginally by AM [19].

Figure 1(b) shows that a similar bandwidth is achieved in the transfer function of f_{rep} and f_{CEO} for pump current modulation, in the order of 10 kHz, limited by the lifetime of the excited state in the Er gain medium coupled with the laser dynamics [9]. The observed bandwidth is comparable to the value previously reported by Washburn *et al.* for the pump diode current-to-comb output power transfer function in another Er:fiber comb [9] but is smaller than the ≈60 kHz roll-off frequency recently reported by Zhang *et al.* for the pump diode current-to-comb amplitude transfer function measured in an Er:fiber comb equipped with an intracavity EOM [15]. One should point out that the laser dynamics and thus the CEO transfer function and bandwidth may slightly depend on the laser mode-locked state, in a similar way as the phase noise PSD was shown to depend on the mode-locking conditions in

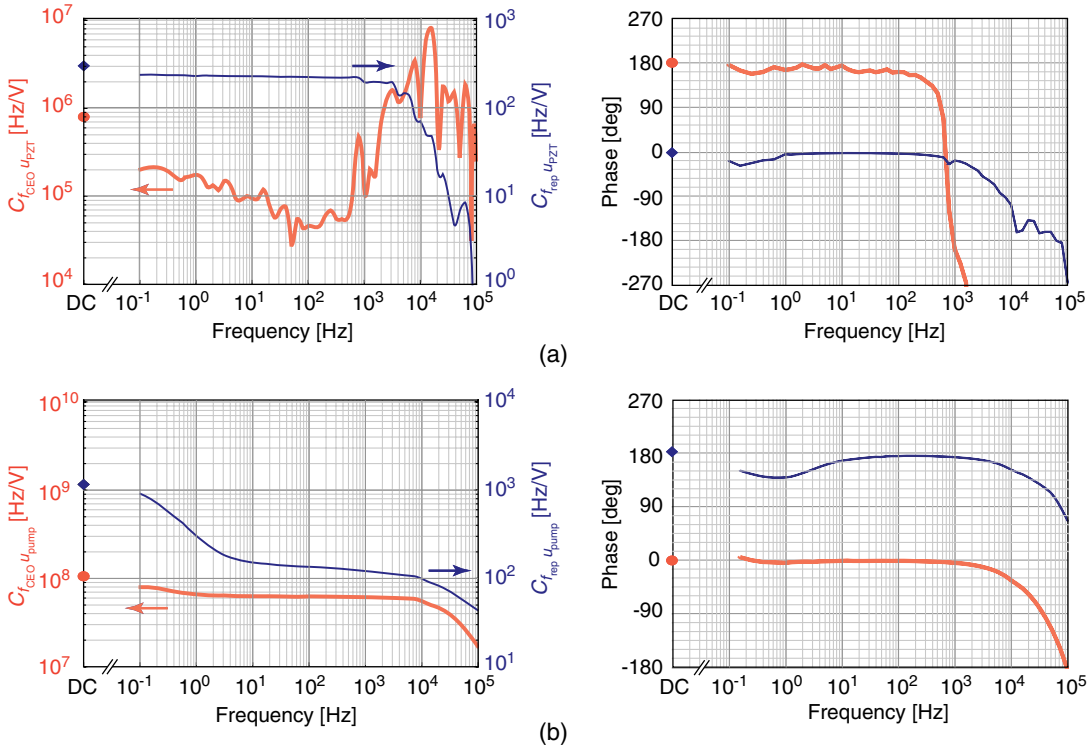

Fig. 1. (Color online) Transfer functions in amplitude (left plots) and phase (right plots) of f_{CEO} (light thick curve, left vertical axis) and f_{rep} (dark thin curve, right vertical axis) in the Er:fiber comb for cavity length modulation, applied through (a) a modulation of the PZT drive voltage and (b) for pump laser modulation. The points on the left vertical axes represent the DC values separately obtained from a static measurement.

an analogous frequency comb [17]. To avoid any issue related to this possible effect, all the measurements reported in this paper have been obtained with the laser operating in the same mode-locked state. At low frequency (below 5 Hz), the behavior significantly differs between f_{rep} and f_{CEO}: a much steeper slope in the amplitude of the f_{rep} transfer function and a significant phase shift are observed. We believe that this effect arises from a thermally induced change of the fiber laser resonator length resulting from the slowly modulated optical power absorbed in the Er-doped fiber.

As an additional verification of the measured dynamic response of f_{rep}, which is potentially the most susceptible to AM-induced artifacts, we also measured the transfer function of an optical comb line with respect to pump laser modulation (1 mV rms applied to the laser driver). This was realized by beating the free-running comb with a 1.56 μm cavity-stabilized ultranarrow-linewidth laser [18] and by analyzing the laser–comb beat note (f_{beat}) with the Miteq frequency discriminator. In order to distinguish between the contribution of the repetition rate and of the CEO in the heterodyne beat, the CEO contribution was first subtracted from the analyzed signal. This was performed by frequency mixing the ≈40 MHz heterodyne beat with the ≈20 MHz CEO beat and subsequently bandpass filtering the CEO-free component at 20 MHz ($f_{beat} - f_{CEO}$), which was demodulated with the Miteq discriminator. With this proper choice of sign, the analyzed CEO-free beat contains N times the frequency modulation of the repetition rate. No AM issue is encountered in this measurement because of the huge enhancement of the FM amplitude compared to the direct measurement of f_{rep}. The perfect correspondence that we observed between the frequency response of the CEO-free laser–comb beat and $N \cdot f_{rep}$ demonstrates the correctness of the measured repetition rate transfer function.

B. Frequency Dependence of the Comb Quasi-Fixed Point

In the elastic tape model of the comb introduced by Telle and co-workers [8], the assumed full correlation between the noise of f_{CEO} and f_{rep} in a free-running frequency comb leads to a breathing motion of the comb around a fixed point N_{fix}, at which the two noise contributions compensate each other. In this model, the fixed point is given by the ratio of the static tuning coefficients of f_{CEO} and f_{rep} with respect to an external perturbations x (e.g., u_{pump} or u_{PZT}):

$$N_{fix}^{x} = -\left(\frac{\partial f_{CEO}}{\partial x}\right) \Big/ \left(\frac{\partial f_{rep}}{\partial x}\right). \tag{2}$$

In most experiments, the comb fixed point for a given external perturbation has been determined quasi-statically, i.e., by applying a square-waveform modulation at low frequency (typically 0.5–1 Hz) and measuring the corresponding change in f_{CEO} and f_{rep} with a frequency counter (typically with 100 ms gate time) [9,10]. In a different approach, Walker *et al.* [20] modulated the pump power in a Ti:sapphire Kerr lens mode-locked laser at a higher (fixed) frequency of 167 Hz and analyzed the effect on the beat note between a tunable Ti:sapphire cw laser and the nearest comb line. By phase-locking the beat note to a 20 MHz reference frequency via feedback to the cavity length of the mode-locked laser, they used the control voltage of the PLL, synchronously detected, as a sensitive measurement of the frequency shift of the optical comb line induced by the pump power modulation.

By tuning the cw laser across the comb spectrum, they measured the change in optical frequency induced by the pump modulation for different comb modes, so as to extract the comb fixed point. But this measurement was performed at a single modulation frequency and the response of both f_{CEO} and f_{rep} to the applied modulation was considered as instantaneous, so that no possible phase shift between f_{CEO} and f_{rep} was accounted for.

Here, our dynamic measurements of the CEO and repetition rate complete transfer functions (in amplitude and phase) over a broad range of modulation frequencies led us to introduce two modifications to the original comb elastic tape model:

(i) The measured transfer functions show that a phase shift might occur between the response of f_{CEO} and f_{rep} to a given modulation. The resulting noise of a comb line of index N can thus be considered as a vector sum of two complex contributions $C_{f_{\mathrm{CEO}}x}(\omega)\cdot\tilde{x}(\omega)$ and $N\cdot C_{f_{\mathrm{rep}}x}(\omega)\cdot\tilde{x}(\omega)$, where the complex dynamic tuning rates are considered here, $C_{fx}=|C_{fx}|e^{i\varphi}$, where φ is the phase of the transfer function and f stands for either f_{CEO} or f_{rep}. This vector sum can be zeroed at a particular value of N ($N=N^{x}_{\mathrm{fix}}$) only in the case of a perfect correlation ($\varphi_{\mathrm{CEO}}-\varphi_{\mathrm{rep}}=0$) or anticorrelation ($\varphi_{\mathrm{CEO}}-\varphi_{\mathrm{rep}}=\pi$) between the response of f_{CEO} and f_{rep} to a given modulation. This corresponds to the traditional fixed point considered in previous studies. In all other cases where $\varphi_{\mathrm{CEO}}-\varphi_{\mathrm{rep}}\neq k\pi$ ($k=0,1,\ldots$), a full compensation of the contributions of $C_{f_{\mathrm{CEO}}x}(\omega)\cdot\tilde{x}(\omega)$ and $N\cdot C_{f_{\mathrm{rep}}x}(\omega)\cdot\tilde{x}(\omega)$ cannot occur, so that a true fixed point does not exist. However, there is still one comb line for which the resulting noise is minimized (but is not zero), and we call the corresponding mode index the quasi-fixed point, which is given by

$$N^{x}_{\text{q-fix}}(\omega)=-\mathrm{Re}\left[\frac{C_{f_{\mathrm{CEO}}x}(\omega)}{C_{f_{\mathrm{rep}}x}(\omega)}\right]. \tag{3}$$

The resulting frequency deviation of an arbitrary comb line ν_N is given by

$$|\Delta\tilde{\nu}_N(\omega)|=|C_{f_{\mathrm{rep}}x}(\omega)\cdot\tilde{x}(\omega)|\sqrt{\left\{\mathrm{Im}\left[\frac{C_{f_{\mathrm{CEO}}x}(\omega)}{C_{f_{\mathrm{rep}}x}(\omega)}\right]\right\}^{2}+(N-N^{x}_{\text{q-fix}}(\omega))^{2}}, \tag{4}$$

showing that a true fixed point exists only if the imaginary part of $C_{f_{\mathrm{CEO}}x}/C_{f_{\mathrm{rep}}x}$ is zero, i.e., $\varphi_{\mathrm{CEO}}-\varphi_{\mathrm{rep}}=k\pi$.

(ii) Our dynamic measurements performed over a broad frequency range enabled us to determine a quasi-fixed point at each Fourier frequency $\omega/2\pi$ of the considered perturbation, and thus to obtain a frequency distribution of the comb quasi-fixed point. Such an approach had not been applied earlier to the best of our knowledge. Kim *et al.* [10] reported a related approach in a Cr:forsterite 1.3 μm comb, but applied to the measurement of the frequency response of a comb line for pump power modulation. They analyzed the frequency response of the heterodyne beat note between a comb line and a narrow-linewidth laser using a delay line frequency discriminator. Performing such a measurement with a couple of lasers at different wavelengths (1319 nm close to the comb fixed point, 1064 and 1550 nm on both sides of the fixed point), they could show a significantly smaller response near the comb fixed point at 1319 nm and a ≈180° phase difference between the frequency response of the 1064 and 1550 nm beat notes, showing the anticorrelation between them. As the analyzed beat note signals contain the combined contributions of both f_{CEO} and f_{rep}, which could not be individually inferred in these measurements, this approach neither accurately determined the position of the comb fixed point (due to the very small number of different considered wavelengths) nor showed any Fourier frequency dependence of the fixed point.

From our separate measurement of the dynamic response of f_{CEO} and f_{rep} in amplitude and phase as reported in Subsection 3.A, the response of any comb line can be processed, which is the strength of our approach. Moreover, this enables us to introduce a frequency-dependent comb quasi-fixed point $N^{x}_{q\text{-fix}}(\omega)$ as shown in Eq. (3).

The frequency-dependent quasi-fixed points obtained for cavity length and pump power modulation are shown in Fig. 2. In the case of cavity length fluctuations, the phase of $C_{f_{\mathrm{CEO}}u_{\mathrm{PZT}}}$ and $C_{f_{\mathrm{rep}}u_{\mathrm{PZT}}}$ is close to 0 and π, respectively, for modulation frequencies ranging from DC to ≈200 Hz. A true fixed point thus arises in this case, varying from $N^{\mathrm{PZT}}_{\mathrm{fix}}\approx 200$ at $\omega/2\pi=200$ Hz to $N^{\mathrm{PZT}}_{\mathrm{fix}}\approx 1{,}000$ at $\omega/2\pi=0.1$ Hz and tending to the DC value of ≈2,600 obtained from the static tuning coefficients of f_{CEO} and f_{rep}. This later value corresponds to an optical frequency $\nu^{\mathrm{PZT}}_{\mathrm{fix}}=N^{\mathrm{PZT}}_{\mathrm{fix}}\cdot f_{\mathrm{rep}}\approx 0.7$ THz, which is close to the value of 1 THz previously reported for the fixed point in another Er:fiber laser [21]. At Fourier frequencies higher than 200 Hz, the phase difference between the transfer functions of f_{CEO} and f_{rep} departs from π, so that only a quasi-fixed point can be defined. This quasi-fixed point cannot be accurately determined because of numerous PZT resonances, which strongly influence the CEO transfer function [see Fig. 1(a)]. The sign reversals in the transfer function of f_{CEO} associated with these resonances lead to a quasi-fixed point

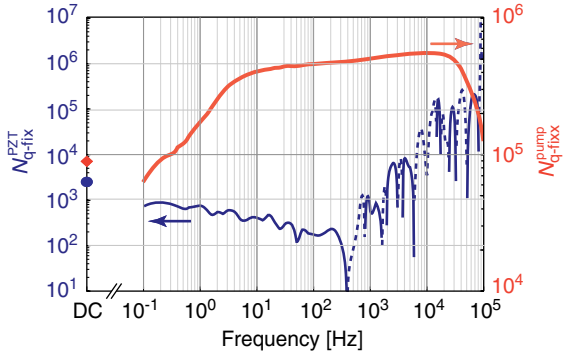

Fig. 2. (Color online) Spectral distribution of the comb quasi-fixed point obtained for cavity length modulation (left vertical scale, thin blue curve) and for laser pump power modulation (right vertical scale, thick red curve). The points on the left vertical axis represent the static fixed points obtained from the ratio of the DC tuning coefficients of f_{CEO} and f_{rep}. The quasi-fixed point for cavity length modulation presents many sign reversals that result from mechanical resonances in the PZT. The solid curve corresponds to positive values of $N^{\mathrm{PZT}}_{q\text{-fix}}$ and the dashed curve to negative values of $N^{\mathrm{PZT}}_{q\text{-fix}}$.

for cavity length fluctuation that alternates between positive and negative values at higher Fourier frequencies.

For pump current modulation, a significant phase shift is observed at a low modulation frequency (below ≈10 Hz) in the transfer functions of f_{rep}. This leads to the absence of a true fixed point, and only a quasi-fixed point can be defined according to Eq. (3). Furthermore, an important increase of the comb quasi-fixed point is observed at low frequency, from the static value $N_{\mathrm{fix}}^{\mathrm{pump}} \approx 9 \cdot 10^4$ and $N_{q\text{-fix}}^{\mathrm{pump}} \approx 6.4 \cdot 10^4$ at $\omega/2\pi = 0.1$ Hz to $N_{q\text{-fix}}^{\mathrm{pump}} \approx 4 \cdot 10^5$ at $\omega/2\pi \approx 5$ Hz. At higher modulation frequencies, the phase difference between the transfer functions of f_{CEO} and f_{rep} remains close to π so that a true fixed point can be considered here, which has a much weaker frequency dependence up to ≈20 kHz. The quasi-fixed point corresponds to a quasi-fixed frequency $\nu_{q\text{-fix}}^{\mathrm{pump}}$ ranging from ≈16.2 THz ($\lambda \approx 19$ μm at $\omega/2\pi = 0.1$ Hz) to ≈140 THz ($\lambda \approx 2.2$ μm at $\omega/2\pi = 20$ kHz), which is located far below the laser carrier (192 THz), especially for low frequency modulation. This is in contrast to previous observations made in other Er:fiber lasers [9,21,22], but also in other types of mode-locked lasers such as Cr:forsterite lasers [10], using a different measurement method based on a low-frequency square waveform modulation and a fast counter. The origin of this discrepancy is not explained, but the possibility that the fixed point moves significantly from the carrier was stated [21].

The observed frequency dependence of the (quasi) fixed point indicates that there is not a true fixed point in the comb either for pump power modulation or for cavity length modulation. This represents a new assessment about the noise distribution in a frequency comb, which has not been previously considered to our knowledge and which is an outcome of our dynamic response measurements.

4. COUPLING BETWEEN THE TWO COMB SERVO LOOPS

In this section, we present the model that we developed to describe the coupled servo loops (Subsection 4.A), and we then show the impact of this coupling on the stabilization of the comb repetition rate (Subsection 4.B).

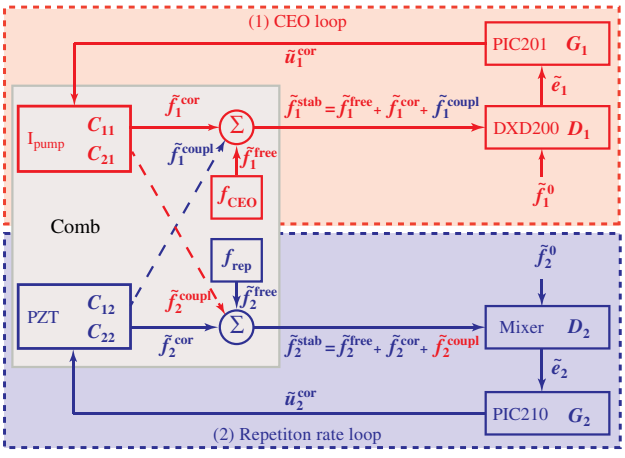

Fig. 3. (Color online) Schematic representation of the two coupled stabilization loops in the Er:fiber comb. Loop (1) stabilizes the CEO frequency and loop (2) the repetition rate.

A. Model of the Coupled Servo-Loops

A fully stabilized optical frequency comb can be schematically described by two interconnected feedback loops, labeled (1) and (2), respectively, as illustrated in Fig. 3. The comb is modeled here by a linear system, which is fully justified as f_{CEO} and f_{rep} were observed to change linearly with the pump power and cavity length, around the considered comb set point, over a broad range compared to the small changes considered in this study. Our model is described in the frequency (Fourier) domain, as is generally done for the description of closed loop transfer functions, and uses the notation commonly adopted to describe laser stabilization loops [23,24]. This approach has two advantages compared to a time domain description. First, it is more pedagogic and intuitive, as it leads to a multiplication of the different transfer functions of the loop components instead of a convolution of the corresponding impulse responses arising in the time domain representation. Second, the noise spectra and transfer functions of the comb are experimentally obtained in the frequency domain.

In the model, loop (1) concerns the stabilization of the CEO frequency and loop (2) the repetition rate. Following the standard description of servo systems [23,24], each loop is composed of the three following elements:

(i) A phase detector, characterized by its transfer function $D_j(\omega)$ in V/Hz. The output of the phase detector constitutes the error signal $\tilde{e}_j(\omega)$, which is proportional to the difference $\delta\tilde{f}_j(\omega)$ between the stabilized input signal frequency $\tilde{f}_j^{\mathrm{stab}}(\omega)$ and the reference frequency $\tilde{f}_j^0$: $\tilde{e}_j(\omega) = D_j(\omega) \cdot \delta\tilde{f}_j(\omega) = D_j(\omega) \cdot (\tilde{f}_j^{\mathrm{stab}}(\omega) - \tilde{f}_j^0)$.

(ii) A servo controller with a transfer function $G_j(\omega)$, which produces a correction signal $\tilde{u}_j^{\mathrm{cor}}(\omega) = G_j(\omega) \cdot D_j(\omega) \cdot \delta\tilde{f}_j(\omega)$.

(iii) An actuator, with a transfer function $C_{jj}(\omega) = C_{f_j u_j}(\omega)$ (in Hz/V), which converts the correction voltage $\tilde{u}_j^{\mathrm{cor}}(\omega)$ into a correction $\tilde{f}_j^{\mathrm{cor}}(\omega) = C_{jj}(\omega) \cdot G_j(\omega) \cdot D_j(\omega) \cdot \delta\tilde{f}_j(\omega)$ of the free-running frequency $\tilde{f}_j^{\mathrm{free}}$.

More specifically, the DXD200 digital phase detector, with a measured transfer function $D_1(\omega) = -e^{-i\pi/2} 1.8 \cdot 10^{-3}/(\omega/2\pi)$ [V/Hz] [19], is used in the CEO stabilization loop. In this case, the actuator is the pump laser current, which is controlled via the voltage $\tilde{u}_1(\omega) = \tilde{u}_{\mathrm{pump}}(\omega)$ applied to the modulation port of the pump laser driver. The pump current corrects the (free-running) CEO frequency $\tilde{f}_1^{\mathrm{free}}$ by $\tilde{f}_1^{\mathrm{cor}}(\omega) = C_{11} \cdot G_1 \cdot D_1 \cdot \delta\tilde{f}_1$, where $C_{11}(\omega) = C_{f_{\mathrm{CEO}} u_{\mathrm{pump}}}(\omega)$. The dependence on the Fourier frequency $\omega/2\pi$ has been omitted here and in the following expressions for the sake of clarity. At the same time, this correction signal changes the repetition rate frequency $\tilde{f}_2^{\mathrm{free}}$ by $\tilde{f}_2^{\mathrm{coupl}}(\omega) = C_{21} \cdot \tilde{u}_1^{\mathrm{cor}}$ (coupling term), where $C_{21}(\omega)$ is the dynamic response of the repetition rate to pump current modulation.

In the repetition rate stabilization loop, a double balanced mixer is used as a phase detector to compare the frequency $(4 \cdot f_{\mathrm{rep}} - f_{\mathrm{DRO}})$ to a 20 MHz reference signal, where f_{DRO} is the frequency of the 980 MHz DRO referenced to the H-maser. The measured transfer function of the phase detector in the repetition rate loop is $D_2(\omega) = -e^{-i\pi/2} 0.86/(\omega/2\pi)$ [V/Hz]. The correction voltage $\tilde{u}_2 = \tilde{u}_{\mathrm{PZT}}$, applied at the input of the high voltage amplifier that drives the PZT of the laser resonator, induces a frequency correction $\tilde{f}_2^{\mathrm{cor}} = C_{22} \cdot G_2 \cdot D_2 \cdot \delta\tilde{f}_2$ of the

free-running repetition rate $\tilde{f}_2^{\text{free}}$, where $C_{22}(\omega)$ is the dynamic response of the repetition rate to cavity length modulation. At the same time, this correction signal changes the CEO frequency $\tilde{f}_1^{\text{free}}$ by a coupling term $\tilde{f}_1^{\text{coupl}} = C_{12} \cdot \tilde{u}_2^{\text{cor}}$, where C_{12} is the dynamic response of the CEO to cavity length modulation.

The coupling between the servo loops is a direct consequence of the nonvanishing tuning coefficients C_{12} and C_{21} that lead to a change of $\tilde{f}_{\text{rep}}$ ($\tilde{f}_{\text{CEO}}$) with a change of $\tilde{u}_{\text{pump}}$ ($\tilde{u}_{\text{PZT}}$). As a result, two terms contribute to the feedback signal applied to the frequency $\tilde{f}_j^{\text{free}}$. In addition to the correction signal $\tilde{f}_j^{\text{cor}}$ produced by the main stabilization loop, a coupling term $\tilde{f}_j^{\text{coupl}}$ originating from the other loop occurs. Following the standard description of servo systems [23,24], the CEO and repetition rate frequencies $\tilde{f}_j^{\text{stab}}(\omega)$ in the fully stabilized comb (closed loops) are related to the free-running frequencies $\tilde{f}_j^{\text{free}}$ (open loops) by

$$\tilde{f}_j^{\text{stab}} = \tilde{f}_j^{\text{free}} + \tilde{f}_j^{\text{cor}} + \tilde{f}_j^{\text{coupl}}. \tag{5}$$

The aforementioned description of the fully stabilized comb constitutes a multiple-input multiple-output system [25]. The feedback signals, made of the direct corrections plus the coupling terms, are obtained from the deviations $\Delta\tilde{f}_j = \tilde{f}_j^{\text{free}} - \tilde{f}_j^{0}$ of the CEO and repetition rate frequencies from their reference values in the free-running frequency comb as

$$\begin{pmatrix} \tilde{f}_1^{\text{cor}} + \tilde{f}_1^{\text{coupl}} \\ \tilde{f}_2^{\text{cor}} + \tilde{f}_2^{\text{coupl}} \end{pmatrix} = \begin{pmatrix} C_{11} & C_{12} \\ C_{21} & C_{22} \end{pmatrix} \cdot \begin{pmatrix} G_1 & 0 \\ 0 & G_2 \end{pmatrix} \cdot \begin{pmatrix} D_1 & 0 \\ 0 & D_2 \end{pmatrix} \cdot \begin{pmatrix} \Delta\tilde{f}_1 \\ \Delta\tilde{f}_2 \end{pmatrix}. \tag{6}$$

Combining Eqs. (5) and (6) and defining $K_j = C_{jj}G_jD_j/(1 - C_{jj}G_jD_j)$, the following expression is obtained for the residual frequency deviations of the fully stabilized optical frequency comb:

$$\delta\tilde{f}_j = \frac{(1+K_j)\left(\Delta\tilde{f}_j + K_k\Delta\tilde{f}_k\frac{C_{jk}}{C_{kk}}\right)}{1 - K_jK_k\frac{C_{jk}C_{kj}}{C_{jj}C_{kk}}}, \tag{7}$$

where $j, k = 1, 2$ and $j \neq k$.

With this model, the residual frequency deviations of the CEO and repetition rate in the fully stabilized frequency comb, $\delta\tilde{f}_j(\omega)$, can be calculated from the frequency deviations of the free-running comb, $\Delta\tilde{f}_j(\omega)$, provided that the gain $K_j(\omega)$ of each loop is known, as well as the comb dynamic response matrix $C_{jk}(\omega)$. Using the definition of the PSD, $S_{xy} = \lim_{T\to\infty}\langle\frac{1}{T}\tilde{x}^*(\omega)\tilde{y}(\omega)\rangle$, we can rewrite Eq. (7) in terms of frequency noise PSD self-spectra (S_{xx}) and cross-spectra (S_{xy}) [26]:

$$\begin{pmatrix} S_{\delta f_1\delta f_1} & S_{\delta f_1\delta f_2} \\ S_{\delta f_2\delta f_1} & S_{\delta f_2\delta f_2} \end{pmatrix} = \begin{pmatrix} H_{11} & H_{12} \\ H_{21} & H_{22} \end{pmatrix}^{+} \cdot \begin{pmatrix} S_{\Delta f_1\Delta f_1} & S_{\Delta f_1\Delta f_2} \\ S_{\Delta f_2\Delta f_1} & S_{\Delta f_2\Delta f_2} \end{pmatrix} \cdot \begin{pmatrix} H_{11} & H_{12} \\ H_{21} & H_{22} \end{pmatrix}, \tag{8}$$

where

$$H_{jj}(\omega) = (1+K_j)\cdot\left(1 - K_jK_k\frac{C_{jk}C_{kj}}{C_{jj}C_{kk}}\right)^{-1},$$

$$H_{jk}(\omega) = (1+K_j)K_k\frac{C_{jk}}{C_{kk}}\left(1 - K_jK_k\frac{C_{jk}C_{kj}}{C_{jj}C_{kk}}\right)^{-1}$$

are the elements of the closed loop transfer function matrix (j, $k = 1, 2$ and $j \neq k$), and the exponent $+$ in the matrix H indicates the Hermitian conjugate. If all the terms on the right-hand side of Eq. (7) or (8) are known experimentally, the resulting noise of the fully stabilized comb [left-hand side of Eq. (7) or (8)] can be calculated and the model can be applied to predict the noise properties of any comb line.

All the matrix elements $C_{jk}(\omega)$ have been measured as described in Subsection 3.B. The additional measurement of the open-loop transfer functions of the phase detectors $D_j(\omega)$ and of the servo controllers $G_j(\omega)$ enabled us to determine all the closed loops transfer functions $H_{jk}(\omega)$. Finally, the frequency noise PSDs of the repetition rate ($S_{\Delta f_2\Delta f_2}$) and of the CEO beat ($S_{\Delta f_1\Delta f_1}$) in the free-running comb have been measured as described in the following sections. However, the cross-spectra $S_{\Delta f_j\Delta f_k}$ ($k \neq j$), which describe the correlation of the noise between the CEO and the repetition rate in the free-running comb, are not known from our experimental measurements.

In the most general case, fluctuations of f_{rep} and f_{CEO} can arise from different noise sources, and thus the correlation between these frequency fluctuations can be only partial. However, we will assume that the fluctuations of f_{CEO} and f_{rep} in the free-running comb are 100% anticorrelated. We will see that this assumption is justified in our case by the measured frequency noise PSD of an optical comb line used to infer some information about the unknown cross-spectra (see Subsection 5.A). This results from the fact that pump power fluctuations constitute the principal source of noise in our free-running comb as discussed later.

The model presented in this section is slightly simplified for ease of understanding and to make it more didactic. The contribution of the noise of the RF references f_j^0 used in the two loops has not been taken into account here, and ideal noiseless references have been considered. This is fully justified for the CEO stabilization loop, as the noise of the stabilized CEO beat is usually orders of magnitude higher than the noise of the reference f_1^0. But the frequency stability of the repetition rate is known to be limited by the noise of the reference when the comb is locked to an RF oscillator [27,28]. Therefore, the noise of the reference f_2^0 used in the repetition rate servo loop has to be taken into account for the completeness of the model, in order to properly determine the noise properties of the repetition rate and, thus, of an optical comb line. An extended model including the noise of the RF reference is detailed in Appendix A. All the results discussed in Subsections 4.B and 5.B have been obtained from this complete model, i.e., using Eqs. (A2)–(A8).

B. Impact of the CEO Stabilization on the Repetition Rate

Our model of the fully stabilized optical frequency comb with two feedback loops shows the cross-impact of the actuators that results from the nonvanishing coupling coefficients $C_{jk}(\omega)$ in Eqs. (7) and (8). In order to observe the influence of this coupling experimentally, we measured the frequency noise PSD of the repetition rate and of the CEO beat in our

Er:fiber comb in two different conditions. In the first case, only one comb parameter was stabilized (either f_{rep} or f_{CEO}) by closing the corresponding loop. The second loop was disabled, so that no signal was applied to the second actuator and thus no coupling occurred. In the second case, both feedback loops were simultaneously enabled, so that their reciprocal coupling influence was observed. In both cases, the frequency noise PSD of the repetition rate and of the CE -beat was measured as described below.

The frequency noise of the repetition rate was measured by detecting the sixth harmonic of f_{rep} at 1.5 GHz using an independent, out-of-loop, fast photodiode (New-Focus 1434, 25 GHz bandwidth). This signal was filtered, amplified, and frequency divided by 15 to be measured against a low-phase-noise 100 MHz synthesizer (SpectraDynamics Cs-1) using a phase noise measurement system (NMS from SpectraDynamics). As an alternative, to overcome the noise floor of the phase noise measurement system occurring at high Fourier frequency, a second measurement was implemented using the HF2PLL frequency discriminator to demodulate the repetition rate. To increase the measurement sensitivity to the small frequency fluctuations of the repetition rate, a higher harmonic of f_{rep} has been used here, i.e., the 12th harmonic at 3 GHz. The HF2PLL frequency discriminator was operated with a 20 MHz carrier frequency. For this purpose, the 3 GHz repetition rate harmonic was frequency downconverted to 20 MHz by mixing with a reference signal at 2.98 GHz delivered by a frequency synthesizer referenced to an H-maser. The low-pass filtered 20 MHz signal was then demodulated in the digital HF2PLL discriminator, and the demodulated signal was measured with an FFT spectrum analyzer. The data obtained with the two measurement systems were combined in order to minimize the limitation due to the instrumental noise floor. The resulting frequency noise spectra are displayed in Fig. 4, together with the frequency of the free-running repetition rate to assess the effect of each actuator. The instrumental noise floor limits the measurement of the repetition rate in the range 10–100 kHz when the CEO is free-running, but in a larger range of 2–100 kHz when the CEO is stabilized.

Whereas the noise of the repetition rate is strongly reduced by the PZT feedback signal, the bandwidth of this servo loop is limited by the transfer function of the PZT to a few hundred hertz. This bandwidth might be enlarged to the kilohertz range, but with the detrimental consequence of a degradation of the optical linewidth of the comb lines due to the larger contribution of the repetition rate servo bump to the comb frequency noise PSD. The repetition rate servo bandwidth was thus limited to a lower value to prevent this degradation. With only the repetition rate loop enabled, the frequency noise around 100 Hz is slightly higher than in the free-running comb as a result of the ≈120 Hz servo bump. A significant improvement in the frequency noise of the repetition rate is observed when the CEO stabilization is enabled. The improvement is larger than one order of magnitude in terms of PSD in the frequency range 60 Hz–4 kHz (however, the measurement with the stabilized CEO is limited by the instrumental noise floor at $\omega/2\pi > 3$ kHz). This results from the cross-sensitivity of f_{rep} to the pump power and to the larger bandwidth of the CEO servo loop. These two features lead to an enhancement of the overall repetition rate feedback bandwidth. As a consequence, the noise of an optical comb line, which is dominated by the noise contribution of the repetition rate, is improved by the CEO stabilization loop (apart from the CEO servo bump at around 10 kHz). In this context, the full stabilization of the comb is beneficial for beat note experiments with external lasers, as it leads to improved noise properties in comparison with the alternative method, where the CEO is not controlled or only very smoothly controlled and then subtracted from the beat note [17]. This fact has been verified experimentally.

We also measured the frequency noise PSD of the CEO beat, with the repetition rate servo loop both enabled and disabled, to observe the influence of the repetition rate stabilization onto the CEO. The frequency noise of the stabilized CEO beat was measured from the signal of the in-loop DXD200 phase detector, recorded with an FFT spectrum analyzer, whereas the frequency noise of the free-running CEO beat was measured using the Miteq frequency discriminator. We observed no significant impact of the repetition rate stabilization on the CEO frequency noise.

These experimental results have been used to check our theoretical model. In Fig. 5, we compare the frequency noise of the repetition rate experimentally measured in the fully stabilized comb with the one calculated with the model [using Eqs. (A2)–(A8)] from the frequency noise of the free-running comb. The experimental results are in a very good agreement

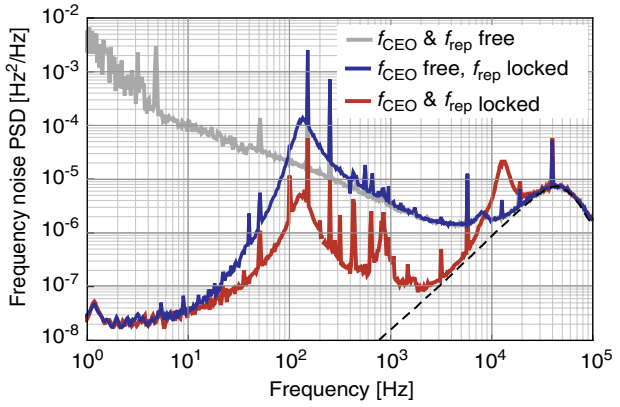

Fig. 4. (Color online) Measured frequency noise PSD of the repetition rate (@250 MHz) in the free-running and stabilized Er:fiber comb (with and without CEO stabilization). At high frequencies, the measurement is limited by the instrumental noise floor of the HF2PLL discriminator (dashed line).

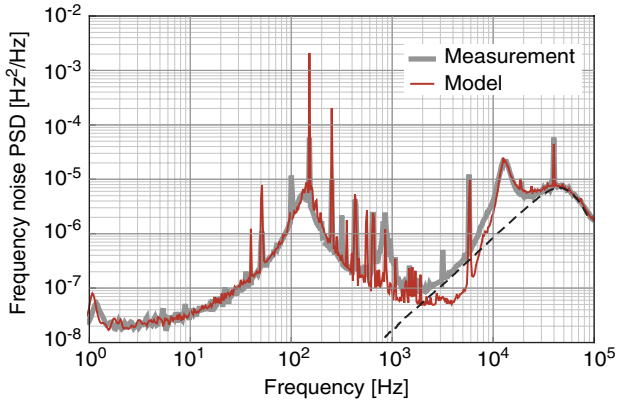

Fig. 5. (Color online) Frequency noise PSD of the repetition rate in the fully stabilized Er:fiber comb: comparison between the experimental measurement (thick grey curve) and the calculation from the theoretical model (thin dark curve).

with the model. The small difference observed in the range 2–10 kHz results from the instrumental noise floor in the measurement of the repetition rate frequency noise. The repetition rate frequency noise measurement is limited by the instrumental noise floor above ≈2 kHz in the fully stabilized comb (see Fig. 4), but in a narrower frequency range (10–100 kHz) for the free-running repetition rate, which is relevant for the spectrum calculated from the model, due to its higher noise.

These experimental results demonstrate the suitability of our theoretical approach in the calculation of the coupling between the repetition rate and CEO stabilization loops. In the next section, we will present a further verification of the model applied to the noise of an optical comb line at 1.56 μm.

5. NOISE OF AN OPTICAL COMB LINE

In this section, the developed model is applied to quantify the impact of the servo-loop coupling on the noise properties of the comb. The contribution of the CEO to the frequency noise of a comb line is first shown (Subsection 5.A), then the impact of the servo-loop coupling is assessed by calculating the frequency noise of a comb line in the presence and absence of coupling (Subsection 5.B).

A. CEO Contribution to the Optical Frequency Noise

To assess the impact of the servo-loop coupling on the noise properties of an optical comb line, the heterodyne beat between the comb and a 1.56 μm cavity-stabilized ultranarrow-linewidth laser [18] was characterized. The beat signal was measured with a fiber-coupled photodiode by combining ≈1 mW from the ultrastable laser with ≈60 μW from the comb, spectrally filtered to a 0.3 nm (40 GHz) width using a diffraction grating. About 160 comb lines contribute to the detected comb optical power, corresponding to an average power of less than 400 nW per comb line. Despite this low power, a beat signal with a signal-to-noise ratio of more than 30 dB (at 100 kHz resolution bandwidth) was detected in the range 20–40 MHz depending on the laser fine tuning. The beat note was amplified to ≈0 dBm, bandpass filtered at 20 MHz and then demodulated with the Miteq frequency discriminator. The noise of the demodulated beat signal was recorded with an FFT spectrum analyzer and converted into frequency noise using the discriminator sensitivity. The frequency noise PSD of the heterodyne beat signal represents the frequency noise of the optical comb line as the contribution of the ultranarrow-linewidth laser is negligible.

Figure 6 displays the measured frequency noise PSD of the 1.56 μm comb line and of the CEO beat for comparison (measured from the in-loop DXD200 phase detector as described in Subsection 4.B). One observes that the CEO frequency noise is significantly higher than the noise of the comb line in the range 3–100 kHz, corresponding to the CEO servo bump. This is possible only if the frequency noise of f_{CEO} is anticorrelated and of similar amplitude to the contribution of $N \cdot f_{\mathrm{rep}}$, as the total fluctuation of the comb line ν_N corresponds to $\delta\nu_N = \delta f_{\mathrm{CEO}} + N \cdot \delta f_{\mathrm{rep}}$, which arises from the well-known comb equation $\nu_N = f_{\mathrm{CEO}} + N \cdot f_{\mathrm{rep}}$. In order to verify this statement, the contribution of the CEO beat to the optical comb line was subtracted from the laser–comb heterodyne beat as explained in Subsection 3.A. The CEO-free beat signal, demodulated with the Miteq frequency discriminator and measured with an FFT spectrum analyzer, simply represents the noise of the repetition rate multiplied to the optical domain by the mode number N (i.e. $S_{N\cdot\delta f_{\mathrm{rep}} N\cdot\delta f_{\mathrm{rep}}}$). The similar noise feature observed at 10 kHz for both f_{CEO} and $N \cdot f_{\mathrm{rep}}$, resulting from the servo-loop coupling, confirms that the CEO frequency noise is anticorrelated with the noise of the repetition rate. This leads to a strong reduction of the CEO contribution in the noise of the optical comb line. This anticorrelation is also in agreement with the inverse sign obtained in the static tuning coefficients of f_{CEO} and f_{rep} for pump current variation reported in Subsection 3.A. Comparing the experimentally measured frequency noise PSD of the CEO-free beat ($S_{N\cdot\delta f_{\mathrm{rep}} N\cdot\delta f_{\mathrm{rep}}}$) with the frequency noise PSD of the repetition rate ($S_{\delta f_{\mathrm{rep}}\delta f_{\mathrm{rep}}}$) calculated from our model and multiplied by N^2 shows again very good agreement, as shown in Fig. 7.

B. Impact of the Servo-Loop Coupling

It was experimentally shown in the previous section that the coupling between the CEO and the repetition rate servo loops leads to a strong reduction of the noise of an optical comb line in the 1.5 μm wavelength range. The beneficial influence of the

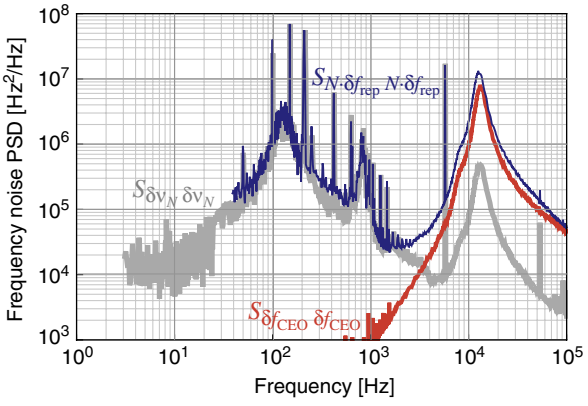

Fig. 6. (Color online) Measured individual contributions of the CEO and repetition rate frequency noise PSD ($S_{\delta f_{\mathrm{CEO}}\delta f_{\mathrm{CEO}}}$ and $S_{N\cdot\delta f_{\mathrm{rep}} N\cdot\delta f_{\mathrm{rep}}}$) to an optical comb line at 1.56 μm and comparison with the measured frequency noise of the optical comb line ($S_{\delta\nu_N\delta\nu_N}$) experimentally assessed from the heterodyne beat with a cavity-stabilized laser.

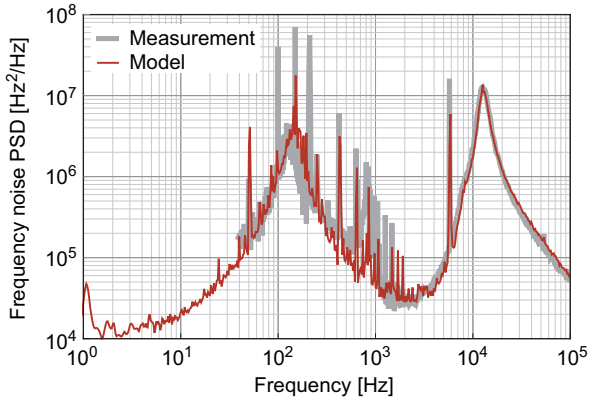

Fig. 7. (Color online) Comparison of the frequency noise of the CEO-free heterodyne beat ($\nu_N - f_{\mathrm{CEO}} = N \cdot f_{\mathrm{rep}}$) experimentally measured (thick grey curve) and calculated from the model (thin dark curve). In order to overcome the limitation in the frequency noise of the free-running repetition rate used in the model that results from the instrumental noise floor (see Fig. 5), the frequency noise PSD of f_{rep} was obtained from the CEO-free optical beat at 1.56 μm ($N \cdot f_{\mathrm{rep}}$ with $N \approx 770{,}000$) divided by N^2.

servo-loop coupling on the comb noise can be quantified with our model by comparing the frequency noise computed in the presence and absence of coupling. However, this procedure is less straightforward than the calculation presented in Subsection 5.A for the CEO-free comb line, where only the noise of the repetition rate ($N \cdot f_{\mathrm{rep}}$) was contributing. Here, the frequency noise of both f_{rep} and f_{CEO} in the free-running comb [i.e., $\Delta\tilde{f}_{\mathrm{rep}}(\omega)$ and $\Delta\tilde{f}_{\mathrm{CEO}}(\omega)$] must be accounted for to determine their resulting noise in the fully stabilized comb, $\delta\tilde{f}_{\mathrm{rep}}(\omega)$ and $\delta\tilde{f}_{\mathrm{CEO}}(\omega)$, using Eqs. (A2)–(A8), and then these quantities must be combined with their respective phase to determine the resulting noise of a comb line $\delta\tilde{\nu}_N(\omega) = \delta\tilde{f}_{\mathrm{CEO}}(\omega) + N \cdot \delta\tilde{f}_{\mathrm{rep}}(\omega)$. In these processes, the correlation between the noise of f_{rep} and f_{CEO} has to be taken into account for a correct application of the model. This can be done either using the cross-spectra $S_{\Delta f_j \Delta f_k}$ in Eq. (8) or by knowing the phase of the frequency deviations $\Delta\tilde{f}_j$ of the free-running comb in Eq. (7) and later on in the stabilized comb ($\delta\tilde{f}_j$). However, none of these parameters is known in our experiments, as only PSD spectra (self-spectra) have been measured for the CEO and repetition rate frequencies. As mentioned in Subsection 4.A, a 100% anticorrelation between $\Delta\tilde{f}_{\mathrm{rep}}(\omega)$ and $\Delta\tilde{f}_{\mathrm{CEO}}(\omega)$ has been considered when applying the model to the noise of an optical comb line, and we will justify this assumption here.

To infer the correlation between the noise of the CEO and repetition rate in the free-running comb, the basic comb equation enables the frequency deviation of an optical comb mode to be related to the frequency deviations of the CEO and repetition rate: $\Delta\tilde{\nu}_N = \Delta\tilde{f}_{\mathrm{CEO}} + N \cdot \Delta\tilde{f}_{\mathrm{rep}}$. This can be written down in terms of the frequency noise PSDs as

$$S_{\Delta\nu_N\Delta\nu_N} = S_{\Delta f_{\mathrm{CEO}}\Delta f_{\mathrm{CEO}}} + S_{N\cdot\Delta f_{\mathrm{rep}}N\cdot\Delta f_{\mathrm{rep}}} + S_{\Delta f_{\mathrm{CEO}}N\cdot\Delta f_{\mathrm{rep}}} + S_{N\cdot\Delta f_{\mathrm{rep}}\Delta f_{\mathrm{CEO}}},$$

where the cross-spectra $S_{\Delta f_{\mathrm{CEO}}N\cdot\Delta f_{\mathrm{rep}}}$ and $S_{N\cdot\Delta f_{\mathrm{rep}}\Delta f_{\mathrm{CEO}}}$ can be replaced by self-spectra using the complex coherence defined in the general case as $\gamma_{xy}(\omega) = S_{xy}(\omega)/\sqrt{S_{xx}(\omega)\cdot S_{yy}(\omega)}$. The resulting frequency noise PSD of the free-running optical comb line is given by the following expression:

$$S_{\Delta\nu_N\Delta\nu_N} = S_{\Delta f_{\mathrm{CEO}}\Delta f_{\mathrm{CEO}}} + S_{N\cdot\Delta f_{\mathrm{rep}}N\cdot\Delta f_{\mathrm{rep}}} + (\gamma_{\Delta f_{\mathrm{CEO}}N\cdot\Delta f_{\mathrm{rep}}} + \gamma_{N\cdot\Delta f_{\mathrm{rep}}\Delta f_{\mathrm{CEO}}}) \times \sqrt{S_{\Delta f_{\mathrm{CEO}}\Delta f_{\mathrm{CEO}}}\cdot S_{N\cdot\Delta f_{\mathrm{rep}}N\cdot\Delta f_{\mathrm{rep}}}}. \quad (9)$$

The sum of the complex coherences can be determined from Eq. (9) as

$$\Gamma_\Delta(\omega) = \gamma_{\Delta f_{\mathrm{CEO}}N\cdot\Delta f_{\mathrm{rep}}} + \gamma_{N\cdot\Delta f_{\mathrm{rep}}\Delta f_{\mathrm{CEO}}} = \frac{S_{\Delta\nu_N\Delta\nu_N} - S_{\Delta f_{\mathrm{CEO}}\Delta f_{\mathrm{CEO}}} - S_{N\cdot\Delta f_{\mathrm{rep}}N\cdot\Delta f_{\mathrm{rep}}}}{\sqrt{S_{\Delta f_{\mathrm{CEO}}\Delta f_{\mathrm{CEO}}}\cdot S_{N\cdot\Delta f_{\mathrm{rep}}N\cdot\Delta f_{\mathrm{rep}}}}}. \quad (10)$$

The frequency noise PSDs of the 1.56 µm comb line, of the CEO beat, and of the CEO-free beat (representing the repetition rate contribution to the frequency noise of the optical comb mode) in the free-running comb, measured as described in Subsection 4.B, are shown in Fig. 8(a). From these spectra, the sum of the complex coherences has been calculated according to Eq. (10) and is displayed in Fig. 8(b) as a function of the Fourier frequency. We observe that the sum of the coherences remains nearly constant at a value of $\Gamma_\Delta(\omega) = \gamma_{\Delta f_{\mathrm{CEO}}N\cdot\Delta f_{\mathrm{rep}}} + \gamma_{N\cdot\Delta f_{\mathrm{rep}}\Delta f_{\mathrm{CEO}}} \approx -2$ in a wide frequency range of 10 Hz–100 kHz. As $|\gamma_{xy}(\omega)| \le 1$, this is only possible if the CEO and repetition rate fluctuations in the free-running optical frequency comb are 100% anticorrelated, which confirms our hypothesis made in Subsection 4.A. One should point out that this observation is not in contradiction with the frequency-dependent comb fixed point that we introduced in Subsection 3.B. Here, the observed value of the coherence sum $\Gamma_\Delta(\omega)$ just tells us how the phases of the fluctuations of f_{CEO} and f_{rep} in the free-running comb are related to each other, but it does not indicate anything about their relative amplitude. On the other hand, the frequency dependence of the comb fixed point that was shown in Fig. 2 is only related to the varying relative amplitude of the transfer functions of f_{CEO} and f_{rep} for a given modulation, not to their phase. Therefore, a frequency-dependent fixed point may occur when the noise in f_{CEO} and f_{rep} is fully correlated. The existence of a quasi-fixed point instead of a fixed point is, however, due

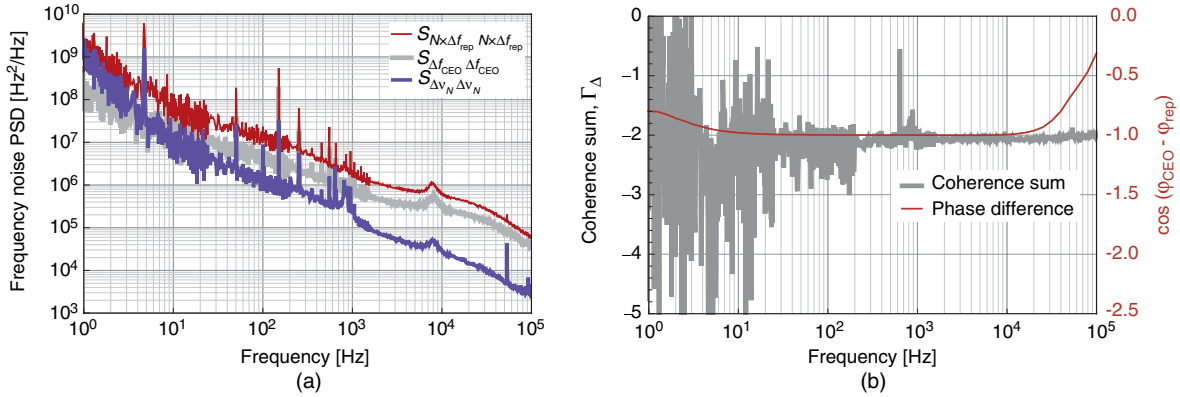

Fig. 8. (Color online) (a) Measured individual contributions of the CEO and repetition rate frequency noise PSDs ($S_{\Delta f_{\mathrm{CEO}}\Delta f_{\mathrm{CEO}}}$ and $S_{N\cdot\Delta f_{\mathrm{rep}}N\cdot\Delta f_{\mathrm{rep}}}$) to an optical comb line at 1.56 µm and comparison with the measured frequency noise of the optical comb line ($S_{\Delta\nu_N\Delta\nu_N}$) experimentally assessed from the heterodyne beat between a cavity-stabilized laser and the free-running comb. (b) Frequency dependence of the sum of the complex coherences $\Gamma_\Delta(\omega) = (\gamma_{\Delta f_{\mathrm{CEO}}N\cdot\Delta f_{\mathrm{rep}}} + \gamma_{N\cdot\Delta f_{\mathrm{rep}}\Delta f_{\mathrm{CEO}}})$ between the frequency variations of the CEO and repetition rate in the free-running comb (left vertical axis). The correlation between the phase of the variations of f_{CEO} and f_{rep} induced by pump current modulation is also shown, represented by $\cos\{\varphi_{\mathrm{CEO}}(\omega) - \varphi_{\mathrm{rep}}(\omega)\}$ (right vertical axis), where φ_{CEO} and φ_{rep} are the phases of the transfer functions of Fig. 1.

to the phase difference between the modulation of f_{CEO} and f_{rep}, $\varphi_{CEO} - \varphi_{rep} \neq k\pi$. In Fig. 8(b), we also plotted the cosine of the phase difference $(\varphi_{CEO} - \varphi_{rep})$ obtained for pump power modulation, for comparison with the coherence sum $\Gamma_\Delta(\omega)$ assessed from the PSDs. Good agreement between these two curves is observed up to ≈10 kHz, even if $\Gamma_\Delta(\omega)$ becomes noisy below ≈30 Hz. This is an indication that pump power fluctuation is the dominant source of noise in our comb, as already pointed out in other Er:fiber combs [15,29]. At higher Fourier frequencies, a discrepancy is observed between $\Gamma_\Delta(\omega)$ and $\cos\{\varphi_{CEO}(\omega) - \varphi_{rep}(\omega)\}$, which seems to indicate that pump fluctuation is no longer the dominant source of noise in the comb, but the anticorrelation between f_{CEO} and f_{rep} remains ($\Gamma_\Delta(\omega) \approx -2$).

In the general model described in Appendix A, we still have to take into account the noise of the RF reference in the repetition rate stabilization loop. When doing so, we lose the information about the phase of the frequency deviations $\delta\tilde{f}_{rep}(\omega)$ of the stabilized repetition rate [see Eq. (A4)], which generally becomes uncorrelated with the CEO deviations $\delta\tilde{f}_{CEO}(\omega)$ within the bandwidth of the repetition rate stabilization loop. For the determination of the residual frequency deviations of an optical comb line in the fully stabilized comb $(\delta\tilde{\nu}_N(\omega))$, we nevertheless considered 100% anticorrelation between $\delta\tilde{f}_{rep}(\omega)$ and $\delta\tilde{f}_{CEO}(\omega)$. This is justified by the following two facts:

(i) At a low Fourier frequency (below a couple of kilohertz), the contribution of the CEO residual noise to a comb line is much smaller than the contribution of the repetition rate $N \cdot \delta\tilde{f}_{rep}(\omega)$ (see Fig. 6), which is limited by the noise $\delta\tilde{f}_2^{ref}(\omega)$ of the RF reference. Therefore, it does not matter if $\delta\tilde{f}_{CEO}(\omega)$ and $N \cdot \delta\tilde{f}_{rep}(\omega)$ are added here in quadrature or by considering a phase relation between these two quantities.

(ii) At a higher Fourier frequency, the noise of the RF reference no longer contributes to $\delta\tilde{f}_{rep}(\omega)$, due to the limited bandwidth of the repetition rate stabilization loop with the PZT. As a consequence, the repetition rate noise is dominated by the CEO servo bump due to the servo-loop coupling, and it is thus highly correlated with $\delta\tilde{f}_{CEO}(\omega)$. This was experimentally confirmed by determining the sum of the complex coherences $\Gamma_\delta(\omega) = \gamma_{\delta f_{CEO} N \cdot \delta f_{rep}} + \gamma_{N \cdot \delta f_{rep} \delta f_{CEO}}$ in the stabilized comb in a similar way to Eq. (10) and Fig. 8(b) for the free-running comb.

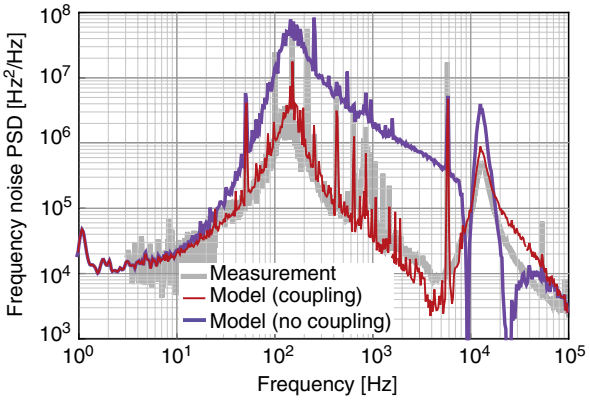

Fig. 9. (Color online) Frequency noise PSD of a comb line at 1.56 μm calculated from the model in the presence and absence of coupling between the two servo loops. The frequency noise spectrum experimentally measured for a 1.56 μm comb line from the heterodyne beat between the comb and an ultrastable laser is also shown for comparison (thick grey curve). In order to overcome the limitation in the frequency noise of the free-running repetition rate used in the model that results from the instrumental noise floor (see Fig. 5), the frequency noise PSD of f_{rep} was obtained from the CEO-free optical beat at 1.56 μm ($N \cdot f_{rep}$ with $N \approx 770{,}000$) divided by N^2.

The frequency noise of the fully stabilized comb was calculated in two different cases, with and without servo-loop coupling. Results are shown in Fig. 9 for a comb line at 1.56 μm. The first case, with the servo-loop coupling taken into account, corresponds to the real behavior of the comb. The calculated spectrum is in good agreement with the frequency noise PSD experimentally measured from the heterodyne beat between the optical frequency comb and the ultrastable laser. This confirms our assumptions about the correlation of the noise of f_{CEO} and f_{rep} in both the unstabilized and stabilized comb. In the second case, nullified coupling coefficients $(C_{jk}(\omega) = 0)$ were considered to simulate the hypothetical case where no coupling would be present between the two servo loops. In that case, the calculated frequency noise PSD of the stabilized comb line is two orders of magnitude higher in a wide Fourier frequency range (100 Hz–10 kHz) than in the presence of coupling. This result demonstrates the positive impact of the cross-influence between the CEO and the repetition rate servo loops on the frequency noise of an optical comb line.

6. DISCUSSION AND CONCLUSION

In order to study the coupled influence of the repetition rate and CEO servo loops in an Er:fiber comb, we first measured the comb dynamic response to a given perturbation, either pump power or cavity length variation. The experimental data led us to introduce two modifications to the elastic tape model originally described by Telle and co-workers [8]. First, we showed that a fixed point does not always exist for a given source of perturbation, and this notion has to be replaced by a quasi-fixed point at which the noise of the comb optical line is minimized but is not zero, due to the incomplete correlation between the fluctuations of f_{CEO} and f_{rep} arising from a phase shift $\varphi_{CEO} - \varphi_{rep} \neq k\pi$ in the dynamic responses of f_{CEO} and f_{rep}. Second, we showed that the quasi-fixed point is not unique for a given source of perturbation but varies with the Fourier frequency of the perturbation instead. All of this experimental evidence led us to extend the former concept of the comb fixed point to a frequency-dependent quasi-fixed point. For cavity length fluctuations, the quasi-fixed point varies by more than one order of magnitude from DC ($N_{fix}^{PZT} \approx 2{,}600$) to 200 Hz Fourier frequency ($N_{q\text{-}fix}^{PZT} \approx 200$). The frequency dependence of the quasi-fixed point for pump current modulation is also significant, showing an important increase from $N_{q\text{-}fix}^{pump} \approx 6.4 \cdot 10^4$ at $\omega/2\pi \approx 0.1$ Hz to $N_{q\text{-}fix}^{pump} \approx 4 \cdot 10^5$ at $\omega/2\pi \approx 5$ Hz, followed by weaker frequency dependence from ≈5 Hz up to ≈20 kHz.

Whereas the quasi-fixed point results from the noise correlation between the CEO and repetition rate in a free-running comb, we also studied the influence of this correlation in the fully stabilized comb. This correlation leads to a coupling between the two servo loops used to phase lock the repetition rate and the CEO frequency to a common RF reference using feedback to the cavity length (via a PZT) and to the pump

power, respectively. We experimentally observed that the repetition rate loop (via the PZT) does not induce any noticeable effect on the CEO stabilization. On the other hand, a significant contribution of the CEO loop (via the pump diode current) to the repetition rate stabilization is observed, leading to a 10-fold reduction of the frequency noise PSD of the repetition rate over a wide range of Fourier frequencies (100 Hz–10 kHz) compared to the case where no coupling would occur. We developed a theoretical model that quantifies the impact of the servo-loop coupling on the comb frequency noise. The model has been validated by experimental data obtained through an extensive characterization of the frequency noise properties of the comb, measured for the CEO beat f_{CEO}, the repetition rate f_{rep}, the repetition rate contribution to an optical comb line $N \cdot f_{\mathrm{rep}} = \nu_N - f_{\mathrm{CEO}}$, and a comb line ν_N at 1557 nm. This model enabled us to predict the frequency noise PSD of an optical comb line at 1557 nm in the presence and in absence of coupling between the servo loops. The results of this modeling show a reduction of the frequency noise of the comb line by almost two orders of magnitude in terms of PSD in a wide frequency range due to the beneficial influence of the CEO stabilization, via feedback to the pump diode current, on the noise of the repetition rate. This is a consequence of the fact that the comb noise results primarily from pump power noise, which leads to a strong correlation between the noise of the repetition rate and of the CEO beat. Therefore, reducing the noise of one of the comb parameters with a feedback loop should also affect the second parameter due to the cross-influence. In our experiment no effect of the repetition rate stabilization is observed on the CEO because of the limited feedback bandwidth (around 150 Hz) and the much smaller frequency noise present in the repetition rate as compared to the CEO beat (which makes the corrections induced to the CEO insignificant). On the other hand, the CEO loop has a significant effect on the repetition rate, because of the large correction signal applied to the pump current (which results from the high noise present in the free-running CEO beat and from the much larger bandwidth of the CEO feedback loop, on the order of 12 kHz).

Finally, the model reported here can be extended with minor adaptations to the case of ultrastable microwave generation, when the comb is locked to an optical reference and used as an optical-to-microwave frequency divider [30]. In such a case, the repetition rate stabilization loop can be slightly modified to account for the stabilization of one comb line to an optical reference (ultrastable laser) instead of directly stabilizing the repetition rate to an RF reference.

APPENDIX A: COMPLETE MODEL OF THE COUPLED SERVO LOOPS ACCOUNTING FOR THE NOISE OF THE FREQUENCY REFERENCES

In the model presented in Subsection 4.A, we considered the error signal $\tilde{e}_j = D_j \cdot \delta\tilde{f}_j$ to be proportional to the difference $\delta\tilde{f}_j = \tilde{f}_j^{\mathrm{stab}} - \tilde{f}_j^{0}$ between the stabilized input signal frequency $\tilde{f}_j^{\mathrm{stab}}$ and an ideal reference frequency $\tilde{f}_j^{0}$. There, the noise of this reference frequency was assumed to be negligible compared to the residual frequency noise of the stabilized frequencies $\tilde{f}_j^{\mathrm{stab}}$. In the real case of a reference signal having finite frequency fluctuations $\Delta\tilde{f}_j^{\mathrm{ref}}$ within the PLL bandwidth, these fluctuations are transferred to the stabilized signal frequency. We account for this contribution in our model by introducing a term responsible for the noise of the reference frequency $\Delta\tilde{f}_j^{\mathrm{ref}} = \tilde{f}_j^{\mathrm{ref}} - \tilde{f}_j^{0}$. In this case, the error signal $\tilde{e}_j = D_j \cdot \delta\tilde{f}_j$ is replaced by $\tilde{e}_j = D_j(\tilde{f}_j^{\mathrm{stab}} - \tilde{f}_j^{\mathrm{ref}}) = D^{(j)}(\delta\tilde{f}_j - \Delta\tilde{f}_j^{\mathrm{ref}})$. Here, as previously, $\delta\tilde{f}_j = \tilde{f}_j^{\mathrm{stab}} - \tilde{f}_j^{0}$ represents the deviations from an ideal reference frequency $\tilde{f}_j^{0}$ in the stabilized comb and $\Delta\tilde{f}_j = \tilde{f}_j^{\mathrm{free}} - \tilde{f}_j^{0}$ are the deviations of the CEO and repetition rate frequencies from their reference values $\tilde{f}_j^{0}$ in the free-running frequency comb. Thus, the frequency correction signal $\tilde{f}_j^{\mathrm{cor}} = C_{jj}G_jD_j(\tilde{f}_j^{\mathrm{stab}} - \tilde{f}_j^{\mathrm{ref}})$ and the coupling term $\tilde{f}_j^{\mathrm{coupl}} = C_{jk}\tilde{u}_k^{\mathrm{cor}}$ in Eq. (6) transform into

$$\begin{pmatrix} \tilde{f}_1^{\mathrm{cor}} + \tilde{f}_1^{\mathrm{coupl}} \\ \tilde{f}_2^{\mathrm{cor}} + \tilde{f}_2^{\mathrm{coupl}} \end{pmatrix} = \begin{pmatrix} C_{11} & C_{12} \\ C_{21} & C_{22} \end{pmatrix} \cdot \begin{pmatrix} G_1 & 0 \\ 0 & G_2 \end{pmatrix} \cdot \begin{pmatrix} D_1 & 0 \\ 0 & D_2 \end{pmatrix} \cdot \begin{pmatrix} \Delta\tilde{f}_1 - \Delta\tilde{f}_1^{\mathrm{ref}} \\ \Delta\tilde{f}_2 - \Delta\tilde{f}_2^{\mathrm{ref}} \end{pmatrix}. \tag{A1}$$

In the resulting expression of the frequency deviations $\delta\tilde{f}_j(\omega)$ of the fully stabilized comb, the contributions originating from the noise of the references can be separated from the contributions intrinsic to the comb. This latter term, labeled here $\delta\tilde{f}_j^{\mathrm{comb}}(\omega)$, corresponds to the ideal case encountered with perfect noiseless references, as considered in Section 4. The additional term arising from the noise of the references is labeled $\delta\tilde{f}_j^{\mathrm{ref}}(\omega)$. The total residual frequency deviations are given by $\delta\tilde{f}_j(\omega) = \delta\tilde{f}_j^{\mathrm{comb}}(\omega) + \delta\tilde{f}_j^{\mathrm{ref}}(\omega)$, with the following expression for each noise source:

$$\delta\tilde{f}_j^{\mathrm{comb}} = \frac{(1+K_j)\left(\Delta\tilde{f}_j + K_k\Delta\tilde{f}_k\frac{C_{jk}}{C_{kk}}\right)}{1 - K_jK_k\frac{C_{jk}C_{kj}}{C_{jj}C_{kk}}}, \tag{A2}$$

$$\delta\tilde{f}_j^{\mathrm{ref}} = -\Delta\tilde{f}_j^{\mathrm{ref}}\frac{K_j\left(1+K_k\frac{C_{jk}C_{kj}}{C_{jj}C_{kk}}\right)}{1 - K_jK_k\frac{C_{jk}C_{kj}}{C_{jj}C_{kk}}} - \Delta\tilde{f}_k^{\mathrm{ref}}\frac{K_k(1+K_j)\frac{C_{jk}}{C_{kk}}}{1 - K_jK_k\frac{C_{jk}C_{kj}}{C_{jj}C_{kk}}}. \tag{A3}$$

As follows from the definition of the frequency noise PSD, by multiplying $\delta\tilde{f}_j(\omega) = \delta\tilde{f}_j^{\mathrm{comb}}(\omega) + \delta\tilde{f}_j^{\mathrm{ref}}(\omega)$ by its complex conjugate and simply replacing all the frequency deviations in Eqs. (A1)–(A3) by the corresponding frequency noise PSDs and cross-spectral densities as $\delta\tilde{f}_j^{*}\delta\tilde{f}_k \to S_{\delta f_j \delta f_k}$, $\Delta\tilde{f}_j^{*}\Delta\tilde{f}_k \to S_{\Delta f_j \Delta f_k}$, and $\Delta\tilde{f}_j^{\mathrm{ref}*}\Delta\tilde{f}_k \to S_{\Delta f_j^{\mathrm{ref}} \Delta f_k}$, the experimentally measurable frequency noise PSDs in the fully stabilized optical frequency comb $S_{\delta f_j \delta f_j}$ can be obtained.

This model describes any pair of coupled loops. However, its implementation requires additional information about the phase of the frequency deviations of the free-running comb $\Delta\tilde{f}_j(\omega)$ (or the cross-spectra $S_{\Delta f_j \Delta f_k}$ in terms of PSDs). We thus assume, on one hand, that the CEO noise is of the same origin as the repetition rate noise and these noise contributions are considered as 100% anticorrelated, as justified in Subsection 5.B. On the other hand, the noise contribution from the reference, $\delta\tilde{f}_j^{\mathrm{ref}}(\omega)$, is totally uncorrelated with the intrinsic comb contribution, $\delta\tilde{f}_j^{\mathrm{comb}}(\omega)$. The frequency noise of the stabilized comb is thus determined from Eqs. (A2) and (A3) using the frequency noise PSDs and taking

$\delta\tilde{f}_j^{\mathrm{ref}}(\omega)$ and $\delta\tilde{f}_j^{\mathrm{comb}}(\omega)$ in quadrature to determine the frequency deviations of the stabilized comb:

$$\left|\delta\tilde{f}_j\right| = \sqrt{\left|\delta\tilde{f}_j^{\mathrm{comb}}\right|^2 + \left|\delta\tilde{f}_j^{\mathrm{ref}}\right|^2}. \tag{A4}$$

In terms of PSDs, Eqs. (A1)–(A4) can be written down as

$$S_{\delta f_j} = S_{\delta f_j^{\mathrm{comb}}\delta f_j^{\mathrm{comb}}} + S_{\delta f_j^{\mathrm{ref}}\delta f_j^{\mathrm{ref}}}, \tag{A5}$$

where

$$\begin{pmatrix} S_{\delta f_1^{\mathrm{comb}}\delta f_1^{\mathrm{comb}}} & S_{\delta f_1^{\mathrm{comb}}\delta f_2^{\mathrm{comb}}} \\ S_{\delta f_2^{\mathrm{comb}}\delta f_1^{\mathrm{comb}}} & S_{\delta f_2^{\mathrm{comb}}\delta f_2^{\mathrm{comb}}} \end{pmatrix} = \begin{pmatrix} H_{11} & H_{12} \\ H_{21} & H_{22} \end{pmatrix}^{+} \cdot \begin{pmatrix} S_{\Delta f_1\Delta f_1} & S_{\Delta f_1\Delta f_2} \\ S_{\Delta f_2\Delta f_1} & S_{\Delta f_2\Delta f_2} \end{pmatrix} \cdot \begin{pmatrix} H_{11} & H_{12} \\ H_{21} & H_{22} \end{pmatrix}, \tag{A6}$$

$$\begin{pmatrix} S_{\delta f_1^{\mathrm{ref}},\delta f_1^{\mathrm{ref}}} & S_{\delta f_1^{\mathrm{ref}},\delta f_2^{\mathrm{ref}}} \\ S_{\delta f_2^{\mathrm{ref}},\delta f_1^{\mathrm{ref}}} & S_{\delta f_2^{\mathrm{ref}},\delta f_2^{\mathrm{ref}}} \end{pmatrix} = \begin{pmatrix} H_{11}^{\mathrm{ref}} & H_{12}^{\mathrm{ref}} \\ H_{21}^{\mathrm{ref}} & H_{22}^{\mathrm{ref}} \end{pmatrix}^{+} \cdot \begin{pmatrix} S_{\Delta f_1^{\mathrm{ref}}\Delta f_1^{\mathrm{ref}}} & S_{\Delta f_1^{\mathrm{ref}}\Delta f_2^{\mathrm{ref}}} \\ S_{\Delta f_2^{\mathrm{ref}}\Delta f_1^{\mathrm{ref}}} & S_{\Delta f_2^{\mathrm{ref}}\Delta f_2^{\mathrm{ref}}} \end{pmatrix} \cdot \begin{pmatrix} H_{11}^{\mathrm{ref}} & H_{12}^{\mathrm{ref}} \\ H_{21}^{\mathrm{ref}} & H_{22}^{\mathrm{ref}} \end{pmatrix}, \tag{A7}$$

$$\begin{aligned} H_{jj}(\omega) &= \frac{(1+K_j)}{1-K_jK_k\frac{C_{jk}C_{kj}}{C_{jj}C_{kk}}}, \\ H_{jk}(\omega) = H_{jk}^{\mathrm{ref}}(\omega) &= \frac{(1+K_j)K_k\frac{C_{jk}}{C_{kk}}}{1-K_jK_k\frac{C_{jk}C_{kj}}{C_{jj}C_{kk}}}, \\ H_{jj}^{\mathrm{ref}}(\omega) &= \frac{K_j\left(1+K_k\frac{C_{jk}C_{kj}}{C_{jj}C_{kk}}\right)}{1-K_jK_k\frac{C_{jk}C_{kj}}{C_{jj}C_{kk}}}. \end{aligned} \tag{A8}$$

ACKNOWLEDGMENTS

This work was financed by the Swiss National Science Foundation (SNSF) and by the Swiss Confederation Program NanoTera.ch, which was scientifically evaluated by the SNSF.

REFERENCES

1. T. W. Hänsch, "Nobel lecture: passion for precision," Rev. Mod. Phys. **78**, 1297–1309 (2006).
2. J. Ye, H. Schnatz, and L. W. Hollberg, "Optical frequency combs: from frequency metrology to optical phase control," IEEE J. Sel. Top. Quantum Electron. **9**, 1041–1058 (2003).
3. M. C. Stowe, M. J. Thorpe, A. Pe'er, J. Ye, J. E. Stalnaker, V. Gerginov, and S. A. Diddams, "Direct frequency comb spectroscopy," Adv. At. Mol.Opt. Phys. **55**, 1–60 (2008).
4. M. J. Thorpe, K. D. Moll, R. J. Jones, B. Safdi, and J. Ye, "Broadband cavity ringdown spectroscopy for sensitive and rapid molecular detection," Science **311**, 1595–1599 (2006).
5. B. Bernhardt, A. Ozawa, P. Jacquet, M. Jacquey, Y. Kobayashi, T. Udem, R. Holzwarth, G. Guelachvili, T. W. Hänsch, and N. Picqué, "Cavity-enhanced dual-comb spectroscopy," Nat. Photonics **4**, 55–57 (2010).
6. R. Paschotta, A. Schlatter, S. C. Zeller, H. R. Telle, and U. Keller, "Optical phase noise and carrier-envelope offset of mode-locked lasers," Appl. Phys. B **82**, 265–273 (2006).
7. E. Benkler, H. R. Telle, A. Zach, and F. Tauser, "Circumvention of noise contributions in fiber laser baser frequency combs," Opt. Express **13**, 5662–5668 (2005).
8. H. R. Telle, B. Lipphardt, and J. Stenger, "Kerr-lens, mode-locked lasers as transfer oscillators for optical frequency measurements," Appl. Phys. B **74**, 1–6 (2002).
9. B. R. Washburn, W. C. Swann, and N. R. Newbury, "Response dynamics of the frequency comb output from a femtosecond laser," Opt. Express **13**, 10622–10633 (2005).
10. K. Kim, J. W. Nicholson, M. Yan, J. C. Knight, N. R. Newbury, and S. A. Diddams, "Characterization of frequency noise on a broadband infrared frequency comb using optical heterodyne techniques," Opt. Express **15**, 17715–17723 (2007).
11. L. Hollberg, S. Diddams, A. Bartels, T. Fortier, and K. Kim, "The measurement of optical frequencies," Metrologia **42**, S105–S124 (2005).
12. F. W. Helbing, G. Steinmeyer, J. Stenger, H. R. Telle, and U. Keller, "Carrier–envelope-offset dynamics and stabilization of femtosecond pulses," Appl. Phys. B. **74**, S35–S42 (2002).
13. J. Rauschenberger, T. Fortier, D. Jones, J. Ye, and S. Cundiff, "Control of the frequency comb from a modelocked Erbium-doped fiber laser," Opt. Express **10**, 1404–1410 (2002).
14. N. Newbury and B. Washburn, "Theory of the frequency comb output from a femtosecond fiber laser," IEEE J. Quantum Electron. **41**, 1388–1402 (2005).
15. W. Zhang, M. Lours, M. Fischer, R. Holzwarth, G. Santarelli, and Y. Le Coq, "Characterizing a fiber-based frequency comb with electro-optic modulator," IEEE Trans. Ultrason. Ferroelectr. Freq. Control **59**, 432–438 (2012).
16. H. R. Telle, G. Steinmeyer, A. E. Dunlop, J. Stenger, D. H. Sutter, and U. Keller, "Carrier-envelope offset phase control: a novel concept for absolute optical frequency measurement and ultrashort pulse generation," Appl. Phys. B **69**, 327–332 (1999).
17. W. Zhang, Z. Xu, M. Lours, R. Boudot, Y. Kersalé, A. N. Luiten, Y. Le Coq, and G. Santarelli, "Advanced noise reduction techniques for ultra-low phase noise optical-to-microwave division with femtosecond fiber combs," IEEE Trans. Ultrason. Ferroelectr. Freq. Control **58**, 900–908 (2011).
18. V. Dolgovskiy, S. Schilt, G. Di Domenico, N. Bucalovic, C. Schori, and P. Thomann, "1.5 μm cavity-stabilized laser for ultra-stable microwave generation," in Proceedings of 2011 Joint Conference of the IEEE International Frequency Control and the European Frequency and Time Forum (FCS), San Francisco, USA, May 2–5, 2011 (IEEE, 2011), pp. 1–3.
19. S. Schilt, N. Bucalovic, L. Tombez, V. Dolgovskiy, C. Schori, G. Di Domenico, M. Zaffalon, and P. Thomann, "Frequency discriminators for the characterization of narrow-spectrum heterodyne beat signals: application to the measurement of a sub-hertz carrier-envelope-offset beat in an optical frequency comb," Rev. Sci. Instrum. **82**, 123116 (2011).
20. D. R. Walker, T. Udem, C. Gohle, B. Stein, and T. W. Hänsch, "Frequency dependence of the fixed point in a fluctuating frequency comb," Appl. Phys. B **89**, 535–538 (2007).
21. N. R. Newbury and W. C. Swann, "Low-noise fiber-laser frequency combs," J. Opt. Soc. Am. B **24**, 1756–1770 (2007).
22. N. Haverkamp, H. Hundertmark, C. Fallnich, and H. R. Telle, "Frequency stabilization of mode-locked Erbium fiber lasers using pump power control," Appl. Phys. B **78**, 321–324 (2004).
23. F. Riehle, *Frequency Standards, Basics and Applications* (Wiley, 2004), Chap. 2.
24. O. Svelto, S. Longhi, G. Della Valle, S. Kück, G. Huber, M. Pollnau, H. Hillmer, S. Hansmann, R. Engelbrecht, H. Brand, J. Kaiser, A. B. Peterson, R. Malz, S. Steinberg, G. Marowsky, U. Brinkmann, D. Lo, A. Borsutzky, H. Wächter, M. W. Sigrist, E. Saldin, E. Schneidmiller, M. Yurkov, K. Midorikawa, J. Hein, R. Sauerbrey, and J. Helmcke, "Lasers and coherent light sources," in *Springer Handbook of Lasers and Optics*, F. Träger, ed. (Springer, 2007), pp. 583–936.
25. J. Bechhoefer, "Feedback for physicists: a tutorial essay on control," Rev. Mod. Phys. **77**, 783–836 (2005).
26. E. Rubiola and F. Vernotte, "The cross-spectrum experimental method," http://arxiv.org/abs/1003.0113.

27. D. C. Heinecke, A. Bartels, and S. A. Diddams, "Offset frequency dynamics and phase noise properties of a self-referenced 10 GHz Ti-sapphire frequency comb," Opt. Express **19**, 18440–18451 (2011).
28. S. Schilt, N. Bucalovic, V. Dolgovskiy, C. Schori, M. C. Stumpf, G. Di Domenico, S. Pekarek, A. E. H. Oehler, T. Südmeyer, U. Keller, and P. Thomann, "Fully stabilized optical frequency comb with sub-radian CEO phase noise from a SESAM-modelocked 1.5 μm solid-state laser," Opt. Express **19**, 24171–24181 (2011).
29. J. J. McFerran, W. C. Swann, B. R. Washburn, and N. R. Newbury, "Suppression of pump-induced frequency noise in fiber-laser frequency combs leading to sub-radion f_{ceo} phase excursion," Appl. Phys. B **86**, 219–227 (2007).
30. J. Millo, M. Abgrall, M. Lours, E. M. L. English, H. Jiang, J. Guéna, A. Clairon, S. Bize, Y. Le Coq, G. Santarelli, and M. E. Tobar, "Ultra-low noise microwave generation with fiber-based optical frequency comb and application to atomic fountain clock," Appl. Phys. Lett. **94**, 141105 (2009).